pISSN 1598-298X / eISSN 2384-0749
J Vet Clin 34(5) : 318-324 (2017)
http://dx.doi.org/10.17555/jvc.2017.10.34.5.318

Journal of Veterinary Clinics
www.ksvc.or.kr

Single-Plane Fluoroscopic Three-Dimensional Kinematics of Normal Stifle Joint in Beagle Dogs

Hyungkyoo Kim[†], Jaemin Jeong[†], Jeonhee Seo*, Young-Won Lee, Ho-Jung Choi, Jiyoung Park, Seong Mok Jeong and Haebeom Lee[1]

College of Veterinary Medicine, Chungnam National University, Daejeon 34134, Korea
**R&D center, Dentis Co. Ltd., Dong-gu, Daegu 41065, Korea*

(Received: June 26, 2017 / Accepted: August 11, 2017)

Abstract : The objective of this study was to establish kinematic reference ranges for the femorotibial (FT) joint and the patellofemoral (PF) joint in healthy small-breed dogs by measuring 3D kinematics at the walk. Single-plane fluoroscopy was used to image the stifle joints of five healthy beagle dogs while the dogs were walking. 3D bone models of the femur, patella, and tibia were reconstructed by computed tomography scanning of the beagle dogs' hind limbs. The shape-matching technique was used to measure kinematic data from the fluoroscopic images and the 3D bone models. The cranial translation of the tibia during walking was inversely proportional to the FT joint flexion. There were significant correlations between the patellar motion and the tibial motion. The FT joint flexion had a strong correlation with the patellar proximodistal translation and flexion. Additionally, the tibial mediolateral translation had a strong correlation with the patellar shift and tilt. In this study, normal in vivo 3D FT joint and PF joint kinematics were demonstrated, and the average kinematic parameters were determined in walking beagle dogs.

Key words **:** canine knee kinematics, single-plane fluoroscopy, shape-matching technique, small-breed dog.

Introduction

In the canine stifle joint, the proper range of motion is maintained by the surrounding ligaments and the joint's articulation structure when the dog is bearing weight in the hind limbs. The canine stifle joint is one of the most common locations for orthopedic conditions such as joint instability and anatomical or mechanical axial malalignment. These conditions can cause lameness and subsequently lead to osteoarthritis and altered stifle joint kinematics (4).

Over the past 50 years, the principal goal of orthopedic surgery has been to solve joint instability and return affected joints to their normal function (6). To achieve this goal, it is essential for surgeons to understand the biomechanics of the affected joint and the various surgical techniques that are utilized to treat the joint. Previously, the prognoses for surgical treatments were determined by the surgeon's observations, which was a subjective measurement. Recently, various methods to objectively measure musculoskeletal functions have been discussed. Several clinical methods of objective gait analysis have become available and human biomechanical studies have been published using these research modalities. In veterinary literature, the majority of published biomechanical studies focused on cranial cruciate ligament injuries. Currently, gait analysis is the criterion-referenced standard for determining the influence of orthopedic disorders on joint biomechanics, evaluating the objective functional outcome after orthopedic surgery, and assessing the effectiveness of different surgical techniques (3).

The optoelectrical motion capture system is the most commonly reported technique used for evaluating in vivo gait analysis in dogs (3,5,9). Unfortunately, this system has limitations, including the decreased accuracy of the in vivo measurement of bone joint kinematics and skin movement artifacts errors that decrease data repeatability, thus restricting the systems use to measuring joint flexion-extension motion only (11). Alternatively, gait analysis can be performed using surgically implanted bone markers with a radiographic imaging system (21). This gait analysis technique can result in highly accurate and reproducible results; however, the invasiveness, risks, and discomfort associated with surgical bone marker implantation limits the clinical application of this technique.

Recently, the shape-matching technique has become a popular method to measure kinematics by aligning CT-based three-dimensional bone models with two-dimensional fluoroscopic images. This noninvasive method of measuring kinematics provides accurate results.

In veterinary literature, the majority of the previous kinematic studies were focused on large-breed dogs with orthopedic diseases, especially dogs with cranial cruciate ligament injuries. Using the shape-matching technique, one study measured the normal in vivo kinematic parameters of the canine knee in large-breed dogs (13). To our knowledge, normal in vivo knee kinematic reference ranges for small-breed dogs have not been reported. It is well recognized that kinematics vary with body morphologies such as size, shape, and cadence

[†]These authors contribute equally to this work
[1]Corresponding author.
E-mail : seatiger76@cnu.ac.kr

(6,13).

The objectives of this study were to investigate the in vivo three-dimensional knee kinematics and to establish reference ranges for healthy, small-breed dogs at the walk. The noninvasive shape-matching technique was utilized to measure the kinematics of beagle dogs.

Materials and Methods

Animals

This study was approved by the Chungnam National University Animal Care and Use Committee (No. CNU-00838). Five purpose-bred beagle dogs, 3 to 5 years of age (mean age of 3.6 years), weighing 9.3 to 11.1 kg (mean body weight of 10 kg), and with body condition scores (BCS) from 4 to 6 out of 9 (mean BCS of 4.8) were included in the study. All dogs had normal orthopedic physical examination findings prior to initiation of the study.

Computed tomography

Computed tomography (CT) images of all the beagle dogs' hind limbs were obtained using a 32-detector row CT scanner (Alexion™, Toshiba, Japan). The obtained CT images were used to build three-dimensional bone models of the femur, patella, and tibia. The CT images were used to confirm the results of the orthopedic physical examinations, and no remarkable findings were observed in any of the dogs. Prior to the CT imaging, all the dogs were fasted for at least 8 hours. A standardized anesthetic protocol was used, as follows: 3 mg/kg of alfaxalone (Alfaxan® inj., Jurox Pharm. Co. Ltd., Australia) was administered intravenously, followed by inhaled 1.5 to 2.0% isoflurane (Ifran®, Hana Pharm. Co. Ltd., Korea). The CT scan settings were 120 kV and 150 mA with a 512 × 512 image matrix, a 0.547 × 0.547 pixel spacing, and a 1 mm slice thickness.

3D bone model construction

The 3D bone models of the femur, patella, and tibia were reconstructed using the Mimics software program (Mimics, Materialise, Belgium) (Fig 1).

Fluoroscopic image acquisition

Prior to obtaining the fluoroscopic images, all dogs were trained to ambulate normally on a horizontal motorized

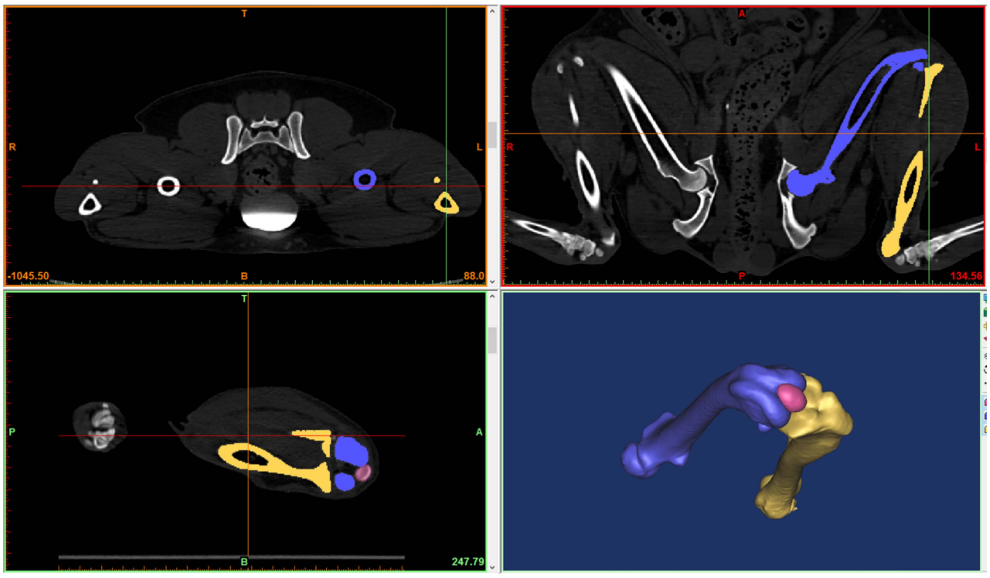

Fig 1. Reconstructed CT-based bone models of the femur, patella, and tibia using the JointTrack software program.

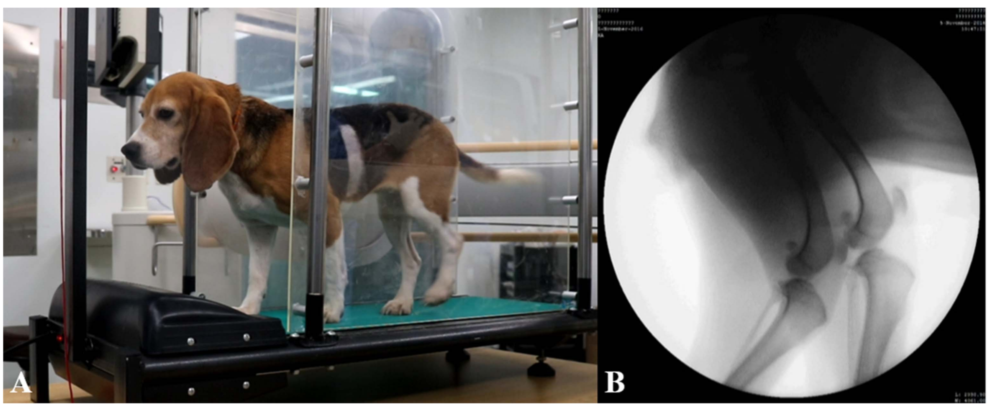

Fig 2. A beagle dog walking on a treadmill to obtain fluoroscopic images (A), Obtained mediolateral view fluoroscopic image (B).

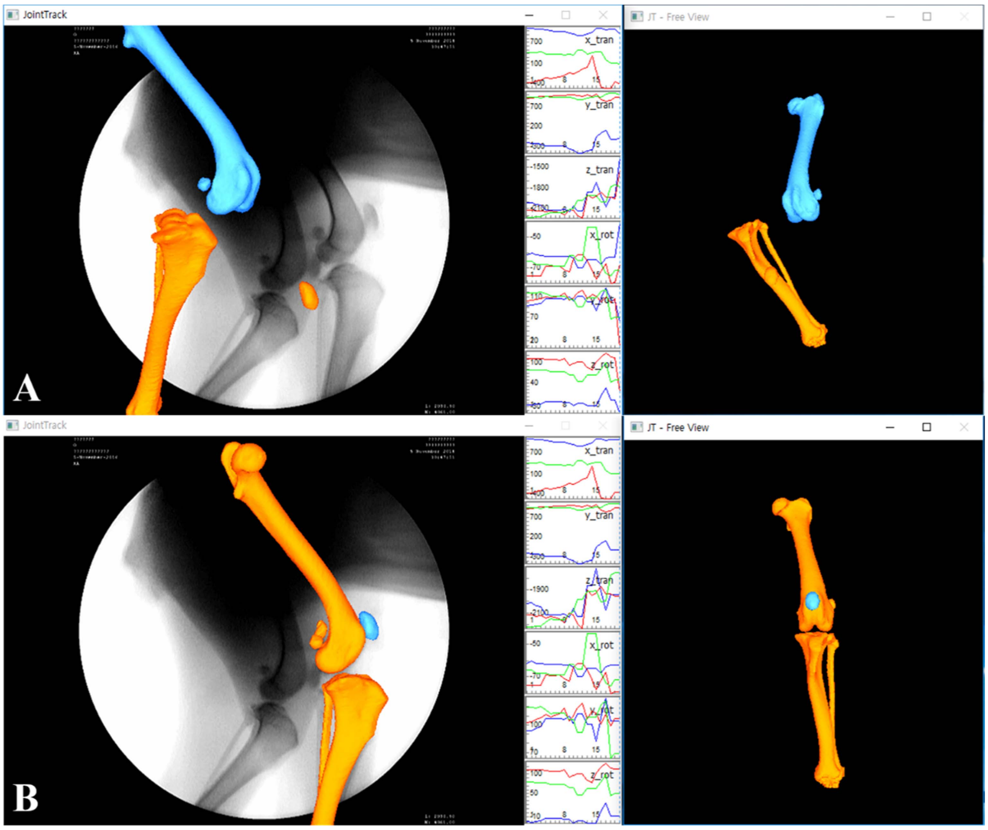

Fig 3. 3D bone models being superimposed on 2D fluoroscopic images by manual manipulation (A), 3D bone models shape-matched after using the software's optimization function (B).

treadmill (Carrydori, CDATA, Korea) without struggling or requiring leash guidance. The dogs were walked on the treadmill for a five to ten minutes session, 2 or 3 sessions per day, every 2 days, for a total of one month.

A commercial, mobile, diagnostic radiograph image acquisition system (BV Pulsera, Philips, Netherlands) at source settings of 52 kVp and 3.86 mAs, with a pulse rate of 30 frames/s and a pulse width of 11.1 ms (Fig 2), was used to acquire the images. Mediolateral view fluoroscopic images of the knees were acquired as the dogs walked on the treadmill.

The velocity of the treadmill was determined according to subject's best ambulation and cadence, with the velocities ranging from 0.2 to 0.3 m/s. Fluoroscopic images were obtained for five full gait cycles. A full gait cycle was defined as paw-strike to ipsilateral paw-strike, as previously described (13).

3D to 2D image matching

The calibration and distortion correction parameters were determined using a calibration image of radiopaque beads in known patterns (Camera Calibration Toolbox for Matlab, The Mathworks Inc., Natick, Massachusetts, USA) and were used to correct all trial images. The corrected images and the 3D bone models based on the CT images were imported into an open source, shape-matching software program (JointTrack, University of Florida: http://sourceforge.net/projects/jointtrack/). The 3D bone models were superimposed on the 2D fluoroscopic images by manually changing the position and orientation of the 3D bone models on the display and using a built-in, automatic, optimizing function in the software program (Fig 3).

Measurement of 3D kinematics

Each gait cycle was time-normalized at 5% intervals from 0 to 100%. Time-normalization allowed for averaging of the data across multiple cycles for individual dogs, despite differences in cadence between trials and between dogs. Of the five gait cycles captured at the walk, the full gait cycle that was subjectively best captured in the field of view was cho-

Table 1. Each Six Degrees of Freedom for Femorotibial Joint and Patellofemoral Joint

Femorotibial Joint			
Translations	Craniocaudal	Proximodistal	Mediolateral
Rotations	Abduction-Adduction	Internal-External	Flexion-Extension
Patellofemoral Joint			
Translations	Craniocaudal	Proximodistal	Shift
Rotations	Rotation	Tilt	Flexion

Fig 4. Femorotibial joint kinematics during walking, average curves.

sen for analysis. The translations and rotations of the femorotibial and patellofemoral joints were measured in 6 Degrees of Freedom (DOF) (Table 1).

Statistical analysis

Data were expressed as the mean ± SD. The graphs show the mean ± SD error bars. Pearson correlations were used to identify the correlations among the kinematic parameters obtained during walking. Statistical analysis was performed using a statistical software program (IBM SPSS Statistics 22.0, SPSS Inc., USA).

Results

Kinematic data for the 6 DOF of the femorotibial and patellofemoral joints in 5 beagle dogs were measured (Figures 4 and 5), and the average knee kinematic parameters were obtained (Table 2).

In the average gait cycle of the five beagles, the stance phase accounted for approximately 66% of the full gait cycle. The extension of the femorotibial joint occurred from the initial stance phase to the early swing phase, and the flexion of the FT joint occurred after completion of 75% of the gait cycle, which was the middle of the swing phase. The range of motion of the flexion-extension angle during walking was 46° (Table 2). The cranial translation of the tibia during walking was inversely proportional to the femorotibial flexion ($r = -0.985$). The tibia translated up to 1.05 mm cranially when the femorotibial joint extended, and the tibia returned to its original position upon flexion of the femorotibial joint.

The distal translation and flexion of the patella showed a strong positive correlation with the flexion of the femorotibial joint ($r = 0.937$, 0.880, respectively). The range of the proximodistal translation and flexion angle of the patella during walking were 0.33 mm and 20°, respectively, while the flexion-extension motion of the femorotibial joint generated an angle range of 40°. The mediolateral shift and tilt of the patella was strongly correlated with the mediolateral translation of the tibia ($r = 0.903$, 0.852, respectively).

Discussion

The present study provides reference ranges and correlations for the kinematic parameters of normal femorotibial and patellofemoral joints in beagle dogs using single-plane fluoroscopy and shape-matching techniques.

In a previous in vivo 3D kinematic study of the canine stifle joint in large-breed dogs during daily activities (13), the increased knee flexion angle was significantly associated with the tibial internal rotation and anterior translation. In this study, the tibial internal rotation was not identified when the knee flexion angle was increased. Additionally, the tibial anterior translation was observed when the femorotibial joint went into extension in the stance phase, which was when the joint was weight bearing. In a previous kinematic study using bone implants and radiostereometric analysis (16), tibial

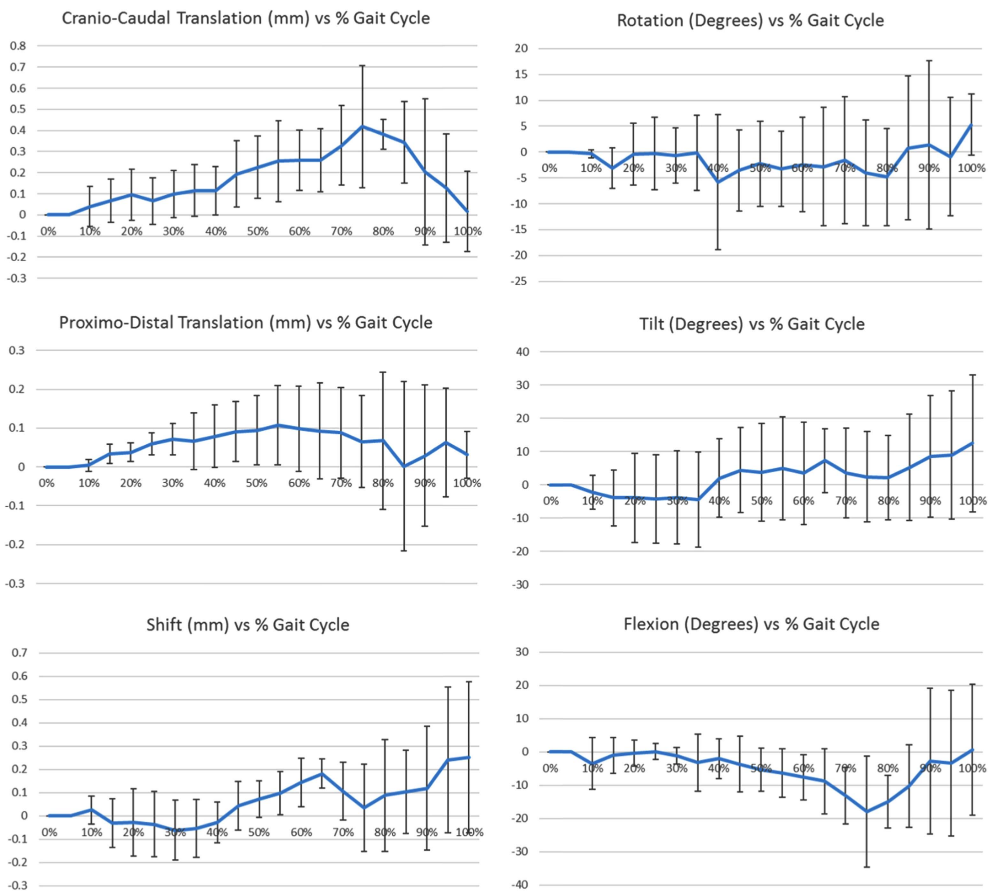

Fig 5. Patellofemoral joint kinematics during walking, average curves.

Table 2. Average Knee Kinematics for all Dogs During Walking

	Femorotibial Joint					
	Cranial Translation	Distal Translation	Medial Translation	Flexion Angle	Abduction Angle	Internal Rotation
Minimum	−0.07 mm (0.11)	−0.11 mm (0.14)	−0.13 mm (0.13)	−41° (8)°	−9° (4)	−4° (3)
Maximum	1.05 mm (0.15)	0.16 mm (0.09)	0.20 mm (0.13)	5° (6)°	5° (4)	11° (4)
Range of Motion	1.12 mm (0.21)	0.26 mm (0.08)	0.33 mm (0.17)	46° (4)°	14° (2)	15° (2)
	Patellofemoral Joint					
	Cranial Translation	Distal Translation	Medial Shift	Flexion	Medial Rotation	Medial Tilt
Minimum	−0.12 mm (0.18)	−0.02 mm (0.03)	−0.13 mm (0.11)	−21° (16)	−5° (0)	−7° (5)
Maximum	0.54 mm (0.21)	0.31 mm (0.22)	0.33 mm (0.20)	14° (14)	10° (8)	21° (14)
Range of Motion	0.66 mm (0.19)	0.33 mm (0.21)	0.46 mm (0.14)	35° (11)	15° (8)	28° (9)

Data in parentheses indicate ± 1 standard deviation.

anterior translation was not observed in normal dogs during walking.

Because the patella is firmly attached to the tibia by the patellar ligament, the femorotibial joint and the patellofemoral joint are known as interdependent (7). In our study, there are significant correlations between patellar motion and tibial motion. The femorotibial flexion had a strong correlation with the patellar proximodistal translation and flexion. Additionally, the tibial mediolateral translation had a strong correlation with the patellar shift and tilt. To our knowledge, there are no kinematic studies that report the motion of patellofemoral joint. One study described the range of motion at the walk and the trot in small-breed dogs with patellar luxation (14).

Medial patellar luxation is a common cause of hind limb lameness in small-breed dogs. Medial patellar luxation may be due to an anatomical abnormality of the hind limbs, such as coxa vara or a diminished anteversion angle. However, its underlying cause is not fully understood and studies suggest many factors could be the cause of the luxation (17,20,22).

In human medicine, various approaches to measure the patellofemoral joint motion have been reported. However, the accurate measurement of in vivo patellofemoral joint motion remains a challenge (2). It is believed that shift, flexion, tilt, and rotation of the patella cause most of the clinical signs of patellar luxation. In human medicine, the anterior-posterior translation and the superior-inferior translation of the patella are less meaningful from a clinical perspective (2).

The kinematic analysis with fluoroscopic shape-matching techniques can be achieved by either single-plane fluoroscopic (SF) analysis or bi-plane fluoroscopic (BF) analysis. Both methods have the major advantage of being noninvasive. BF analysis has been described in humans, and it is more accurate than SF analysis. Despite the higher level of accuracy, the system's high costs and the requirement of a double dose of radiation limits the use of BF analysis. In contrast, SF analysis is cost-effective and requires a lower radiation dose for the same purpose (19).

The present study has several limitations. The kinematic data were obtained using SF analysis, which is less accurate than BF analysis. In one canine cadaveric study, SF analysis error was reported to be within 1.28 mm for translations and 1.58 degrees for rotations (11). In human studies, SF analysis error has been reported to be 1.4 to 5.6 mm for out-of-plane translation and 0.4 to 1.3 degrees for rotations (1,8,10, 12,15,18). The fluoroscopic images used in the present study were mediolateral views, so the accuracy of the kinematic data of motion that was obtained out of the sagittal plane may vary with the actual kinematics of a walking dog. The small number of experimental animals included in the study may not be representative of the entire dog population. Additionally, the experimental animals were from a homogenous Beagle breed population, so the results of this study may not represent the kinematics of other small-breed dogs. Further research is warranted to determine the normal kinematics of the stifle joint in other small-breed dogs.

Conclusion

Using single-plane fluoroscopy, normal in vivo three-dimensional femorotibial joint and patellofemoral joint kinematics were demonstrated in beagle dogs at the walk, and the average kinematic parameters were determined. In beagle dogs, a different kinematic analysis was observed compared to that reported in a previous study using large-breed dogs. Further studies on the knee kinematics and disease conditions in various small-breed dogs are needed to improve understanding of the complexity of this joint.

Acknowledgements

This study was supported by research fund of Chungnam National University.

References

1. Banks SA, Hodge WA. Accurate measurement of three-dimensional knee replacement kinematics using single-plane fluoroscopy. IEEE Trans Biomed Eng 1996; 43: 638-649.
2. Bey MJ, Kline SK, Tashman S, Zauel R. Accuracy of biplane x-ray imaging combined with model-based tracking for measuring in-vivo patellofemoral joint motion. J Orthop Surg Res 2008; 3: 38.
3. Bockstahler BA, Prickler B, Lewy E, Holler PJ, Vobornik A, Peham C. Hind limb kinematics during therapeutic exercises in dogs with osteoarthritis of the hip joints. Am J Vet Res 2012; 73: 1371-1376.
4. Canapp SO. The canine stifle. Clin Tech Small Anim Pract 2007; 22: 195-205.
5. DeCamp CE, Soutas-Little RW, Hauptman J, Olivier B, Braden T, Walton A. Kinematic gait analysis of the trot in healthy greyhounds. Am J Vet Res 1993; 54: 627-634.
6. DeCamp CE. Kinetic and kinematic gait analysis and the assessment of lameness in the dog. Vet Clin North Am Small Anim Pract 1997; 27: 825-840.
7. Evans HE, De Lahunta A. Arthrology. In: Miller's anatomy of the dog, 4th ed. New York: Elsevier. 2013: 178.
8. Fregly BJ, Rahman HA, Banks SA. Theoretical accuracy of model-based shape matching for measuring natural knee kinematics with single-plane fluoroscopy. J Biomech Eng 2005; 127: 692-699.
9. Gillette RL, Angle TC. Recent developments in canine locomotor analysis: a review. Vet J 2008; 178: 165-176.
10. Hoff WA, Komistek RD, Dennis DA, Gabriel SM, Walker SA. Three-dimensional determination of femoral-tibial contact positions under in vivo conditions using fluoroscopy. Clins Biomech 1998; 13: 455-472.
11. Jones SC, Kim SE, Banks SA, Conrad BP, Abbasi AZ, Tremolada G, Lewis DD, Pozzi A. Accuracy of noninvasive, single-plane fluoroscopic analysis for measurement of three-dimensional femorotibial joint poses in dogs. Am J Vet Res 2014; 75: 477-485.
12. Kanisawa I, Banks AZ, Banks SA, Moriya H, Tsuchiya A. Weight-bearing knee kinematics in subjects with two types of anterior cruciate ligament reconstructions. Knee Surg Sports Traumatol Arthrosc 2003; 11: 16-22.
13. Kim SE, Jones SC, Lewis DD, Banks SA, Conrad BP, Tremolada G, Abbasi AZ, Coggeshall JD, Pozzi A. In-vivo three-dimensional knee kinematics during daily activities in dogs. J Orthop Res 2015; 33: 1603-1610.
14. Klinhom S, Chaichit T, Nganvongpanit K. A Comparative Study of Range of Motion of Forelimb and Hind Limb in Walk Pattern and Trot Pattern of Chihuahua Dogs Affected and Non-Affected with Patellar Luxation. Asian J Anim Vet Adv 2015; 10: 247-259.
15. Komistek RD, Dennis DA, Mahfouz M. In vivo fluoroscopic analysis of the normal human knee. Clin Orthop Relat Res 2003; 410: 69-81.
16. Korvick DL, Pijanowski GJ, Schaeffer DJ. Three-dimensional kinematics of the intact and cranial cruciate ligament-deficient stifle of dogs. J Biomech 1994; 27: 77-87.
17. Lavrijsen IC, Leegwater PA, Wangdee C, van Steenbeek FG, Schwencke M, Breur GJ, Meutstege FJ, Nijman IJ, Cuppen E, Heuven HC, Hazewinkel HA. Genome-wide survey indicates involvement of loci on canine chromosomes 7 and 31 in patellar luxation in flat-coated retrievers. BMC Genet 2014; 15: 64.
18. Mahfouz MR, Hoff WA, Komistek RD, Dennis DA. A robust method for registration of three-dimensional knee implant models to two-dimensional fluoroscopy images. IEEE Trans Med Imaging 2003; 22: 1561-1584.
19. Muhit AA, Pickering MR, Ward T, Scarvell JM, Smith PN. A comparison of the 3D kinematic measurements obtained by single-plane 2D-3D image registration and RSA. Conf proc IEEE eng med biol soc 2010; 2010: 6288-6291.
20. Soparat C, Wangdee C, Chuthatep S, Kalpravidh M. Radio-

graphic measurement for femoral varus in Pomeranian dogs with and without medial patellar luxation. Vet Comp Orthop Traumatol 2012; 25: 197-201.

21. Tashman S, Anderst W. In-vivo measurement of dynamic joint motion using high speed biplane radiography and CT: application to canine ACL deficiency. J Biomech Eng 2003; 125: 238-245.
22. Wangdee C, Leegwater PA, Heuven HC, Van Steenbeek FG, Meutstege FJ, Meij BP, Hazewinkel HA. Prevalence and genetics of patellar luxation in Kooiker dogs. Vet J 2014; 201: 333-337.